Tunnel magnetoresistance of 604% at 300 K by suppression of Ta diffusion in CoFeB/MgO/CoFeB pseudo-spin-valves annealed at high temperature

S. Ikeda,[1,a)] J. Hayakawa,[2] Y. Ashizawa,[3,b)] Y. M. Lee,[1,c)] K. Miura,[1,2] H. Hasegawa,[1,2] M. Tsunoda,[3] F. Matsukura,[1] and H. Ohno[1,d)]

[1]*Laboratory for Nanoelectronics and Spintronics, Research Institute of Electrical Communication, Tohoku University, 2-1-1 Katahira, Aoba-ku, Sendai 980-8577, Japan*

[2]*Advanced Research Laboratory, Hitachi, Ltd., 1-280 Higashi-koigakubo, Kokubunji-shi, Tokyo 185-8601, Japan*

[3]*Department of Electronic Engineering, Tohoku University, Sendai 980-8579, Japan*

(Received 30 May 2008; accepted 5 August 2008; published online 29 August 2008)

The authors observed tunnel magnetoresistance (TMR) ratio of 604% at 300 K in $Ta/Co_{20}Fe_{60}B_{20}/MgO/Co_{20}Fe_{60}B_{20}/Ta$ pseudo-spin-valve magnetic tunnel junction annealed at 525 °C. To obtain high TMR ratio, it was found critical to anneal the structure at high temperature above 500 °C, while suppressing the Ta diffusion into CoFeB electrodes and in particular to the CoFeB/MgO interface. X-ray diffraction measurement of MgO on SiO_2 or $Co_{20}Fe_{60}B_{20}$ shows that an improvement of MgO barrier quality, in terms of the degree of the (001) orientation and stress relaxation, takes place at annealing temperatures above 450 °C. The highest TMR ratio observed at 5 K was 1144%. © *2008 American Institute of Physics*. [DOI: 10.1063/1.2976435]

The investigation of magnetic tunnel junction (MTJ) structures with a MgO barrier,[1–5] which realizes high tunnel magnetoresistance (TMR) is important for the development of advanced magnetoresistive random access memories,[6–8] nonvolatile logics,[9–11] and hard disk drives. TMR ratios of up to 500% at room temperature (RT) and 1010% at 5 K, approaching the theoretically predicted value,[12,13] have been observed for sputtered CoFeB/MgO/CoFeB MTJs consisting of pseudo-spin-valve (PSV) stacking structure without antiferromagnetic pinning layer such as MnIr.[10,14] The annealing temperature (T_a=450–525 °C), which results in the maximum TMR ratio for PSV MTJs, is higher than that (T_a=360–425 °C) of the exchange biased-SV MTJs with MnIr layer.[15,16] The main reason for this difference is found to be the absence of diffusion of Mn into the MgO barrier at high T_a above 450 °C. However, the mechanism of the reduction in the TMR ratio at high T_a over 500 °C has not yet been fully clarified. In this study, we investigated the dependence of the TMR ratio on T_a for PSV MTJs with various CoFeB compositions and thicknesses.

The MTJs used in this work have a stacking structure of, from the bottom, thermally oxidized Si wafer/Ta(5)/Ru(10)/Ta(5)/$Co_xFe_{80-x}B_{20}(t_{CoFeB})$/MgO(1.5,2.1)/$Co_xFe_{80-x}B_{20}$(4)/Ta(5)/Ru(5) (in nm). The composition x of Co was varied from 0 to 60 at. %. The bottom CoFeB layer thickness t_{CoFeB} was varied from 2.3 to 6.0 nm. The conditions of MTJ fabrication and TMR measurement have been described elsewhere.[14,15] The film structures were investigated by x-ray diffraction (XRD) using Cu $K\alpha$ radiation and high resolution transmission electron microscopy (HRTEM) with energy dispersive x-ray spectroscopy (EDX).

Figure 1 shows the TMR ratios at RT as a function of T_a for PSV MTJs with 4.0-nm-thick top and 4.3-nm-thick bottom $Co_xFe_{80-x}B_{20}$ electrodes with x ranging from 0% to 60%. In all samples, having different CoFeB compositions, TMR ratio increases with increasing T_a and reaches maximum at T_a ranging from 475 to 500 °C. When all samples are annealed at T_a over 500 °C, TMR ratios saturate and then gradually decrease. The maximum TMR ratio is 500% at RT (1010% at 5 K) for a MTJ with x=25% and a 2.1-nm-thick MgO barrier.[14] High TMR ratio over 400% was observed for MTJs with x=20% and 40%. It has been suggested that the high TMR ratios at T_a above 475 °C are related to the improved quality of MgO barrier,[17,18] in addition to the crystallization of initially amorphous CoFeB to highly oriented bcc (001) textured CoFeB.[4,19,20] Note that CoFeB electrodes start to form bcc (001) textures at a much lower annealing temperature of T_a=325 °C (Refs. 4 and 21) and crystallization is completed before T_a reaches 475 °C. In order to experimentally address the quality of MgO barriers, XRD measurements (out-of-plane ω-2θ scan, rocking curve by ω scan, and in-plane φ-2$\theta\chi$ scan) were performed. Figure

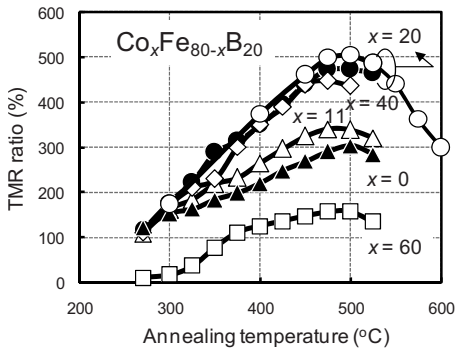

FIG. 1. TMR ratio as a function of annealing temperature for PSV MTJs having $Co_xFe_{80-x}B_{20}$ electrodes with x=0%–60% and t_{CoFeB}=4.3 nm. The MgO thickness of the MTJs is 1.5 nm except for the open circles (2.1 nm).

a)Electronic mail: sikeda@riec.tohoku.ac.jp.
b)Present address: Nihon University, Funabashi 274-8501, Japan.
c)Present address: Fujitsu Laboratories, Ltd., Atsugi 243-0197, Japan.
d)Electronic mail: ohno@riec.tohoku.ac.jp.

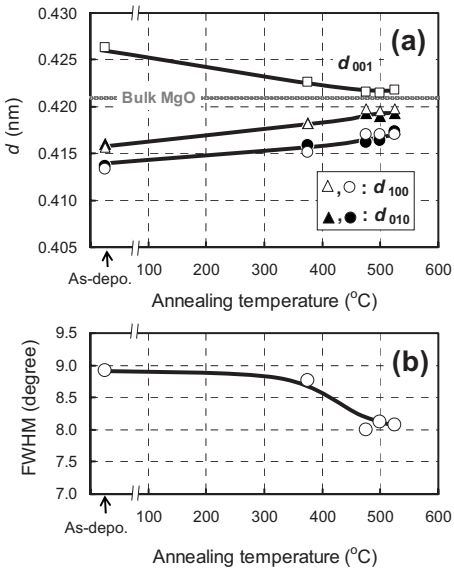

FIG. 2. (a) Lattice parameter d as a function of the annealing temperature for two structure samples with substrate/MgO(10) (open squares, open triangles, and filled triangles) and substrate/Ta(5)/Ru(10)/Ta(5)/$Co_{20}Fe_{60}B_{20}$(3)/MgO(10) (open circles and filled circles). (b) FWHM in the rocking curves of MgO as a function of the annealing temperature for substrate/MgO(10).

2(a) shows the annealing temperature dependence of the lattice parameter d of MgO layer for two structures [substrate/MgO(10) and substrate/Ta(5)/Ru(10)/Ta(5)/$Co_{20}Fe_{60}B_{20}$(3)/MgO(10), which were prepared separately for the XRD study]. d_{001} (open squares) and d_{100} (open circles and triangles) were calculated from the (002) and (200) peaks in ω-2θ and φ-$2\theta\chi$ scan profiles, respectively. d_{010} $(=\sqrt{d_{110}^2 - d_{100}^2}$, filled circles and triangles) was calculated using the (200) and (220) peaks in φ-$2\theta\chi$ scan profiles. Although the thickness and the stack structure of the MgO layers of these samples differ from the actual MgO barrier used in the MTJs, we believe that it still provides valuable information on the morphology of MgO barrier. For both samples, the (001) orientation of MgO was confirmed from the result that the intensity ratio I_{200}/I_{220} was almost 4.[22] In the as-deposited state of MgO directly on substrate, d_{001} expands and d_{100} and d_{010} contract as compared with the bulk value (d=0.421 nm). d_{001} decreases monotonically with T_a, whereas d_{100} and d_{010} increase. A similar tendency was observed in the sample consisting of substrate/Ta(5)/Ru(10)/Ta(5)/$Co_{20}Fe_{60}B_{20}$(3)/MgO(10). Sputtered films are known to have residual stress, which depends on sputtering conditions, depending on the film growth conditions and the atomic peening effect by the sputtering gas.[23] The residual stress of MgO in this case corresponds to compressive stress. As a result of relaxation of stress with the increase in T_a, the lattice parameter approaches a bulk value. In addition, as shown in Fig. 2(b), the full width at half maximum (FWHM) in the rocking curves of the MgO film at (002) decreases with increasing T_a. Note that these analyses of MgO in the special XRD samples do not directly correspond to the structural features of the actual MgO barrier sandwiched by CoFeB electrodes in the MTJs. The structural improvement of MgO may, however, be partly responsible for the enhancement of the TMR ratio after high temperature annealing, although the drop in TMR ratios at T_a over 500 °C observed regardless of the CoFeB compositions cannot be explained

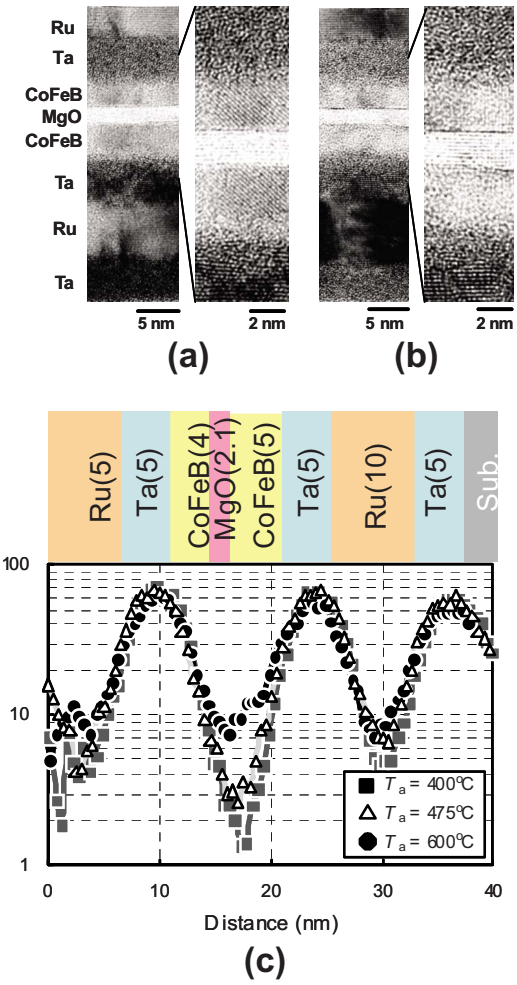

FIG. 3. (Color online) Cross-sectional HRTEM images for PSV MTJs (a) after annealing at 475 °C and (b) after annealing at 600 °C. (c) EDX line profiles of Ta composition after annealing at 400, 475, and 600 °C for substrate/Ta(5)/Ru(10)/Ta(5)/$Co_{20}Fe_{60}B_{20}$(5)/MgO(2.1)/$Co_{20}Fe_{60}B_{20}$(4)/Ta(5)/Ru(5) stack structure.

by these XRD results. To investigate the reasons for the decrease in the TMR ratios at high T_a over 500 °C for the PSV MTJs, HRTEM with EDX was employed for structural characterization. Figure 3 shows the cross-sectional HRTEM images of Ta(5)/Ru(10)/Ta(5)/$Co_{20}Fe_{60}B_{20}$(5)/MgO(2.1)/$Co_{20}Fe_{60}B_{20}$(4)/Ta(5)/Ru(5) films, which were annealed at (a) 475 °C and (b) 600 °C. Two features can be pointed out when the samples were annealed at high temperature of 600 °C: (i) top and bottom CoFeB/Ta interfaces become more indistinct and (ii) the (001) orientation of CoFeB electrodes deteriorates. These structural characteristics observed are consistent with the EDX line analysis in Fig. 3(c), which indicates that Ta diffusion into the CoFeB electrodes and into the MgO barrier becomes noticeable at T_a=600 °C. The diffusion of Ta atoms, having larger atomic radius than Co and Fe atoms, must affect/degrade the quality of CoFeB electrodes and Ta/CoFeB interfaces, which can result in the low TMR ratio of 300% at T_a=600 °C, as seen in Fig. 1. As can be seen in Fig. 3(c), the diffusion of Ta is more pronounced at the bottom CoFeB electrode. This Ta diffusion asymmetry may be caused by the differences in the structure of the top and bottom Ta layers shown in Figs. 3(a) and 3(b). The top Ta layer is amorphous, whereas the bottom Ta layer has a hcp (001) oriented texture, according to the fast Fourier

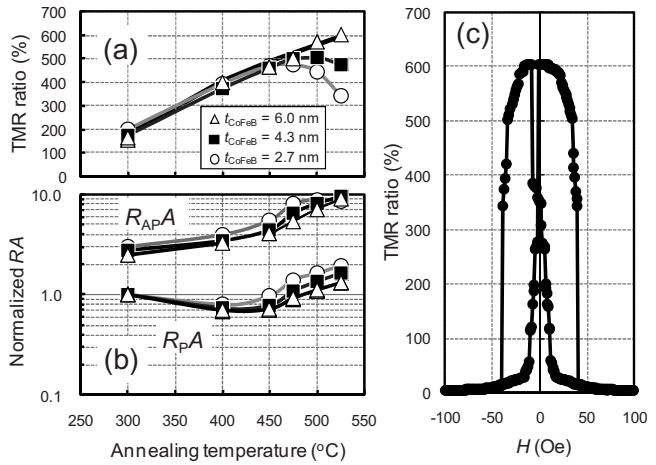

FIG. 4. Annealing temperature dependence of (a) TMR ratio, (b) normalized resistance area products RA (R_PA in parallel magnetization configuration and $R_{AP}A$ in antiparallel magnetization configuration) measured at 300 K for the PSV MTJs with three different bottom $Co_{20}Fe_{60}B_{20}$ thicknesses, t_{CoFeB} =2.7, 4.3, and 6.0 nm. (c) Magnetoresistance loop at 300 K of the PSV MTJ annealed at 525 °C. TMR ratio is as high as 604% at 300 K.

transform of the digitized HRTEM image. These results strongly suggest that even higher TMR ratio may be realized once the Ta diffusion at high annealing temperatures is suppressed. We thus examined below the annealing dependence of MTJs having different bottom CoFeB layer thicknesses, as the diffusion from the bottom Ta layer was more pronounced.

Figures 4(a) and 4(b), respectively, show the TMR ratios and the resistance area products (R_PA in parallel configuration and $R_{AP}A$ in antiparallel configuration) measured at 300 K as a function of T_a for the 2.1-nm-thick MgO barrier PSV MTJs with different bottom CoFeB thicknesses, t_{CoFeB} =2.7 nm (open circles), 4.3 nm (filled squares), and 6.0 nm (open triangles). The R_PA and $R_{AP}A$ in each T_a were normalized by the R_PA of T_a=300 °C, which was around 10^4 Ω μm^2 with no appreciable dependence on t_{CoFeB}. When annealed at T_a of less than 450 °C, the TMR ratios of the three series of MTJs were virtually the same. The effect of bottom CoFeB electrode thickness started to appear at T_a higher than 475 °C. The maximum observed TMR ratio was 604% in a P-SV MTJ having t_{CoFeB}=6.0 nm annealed at 525 °C. A TMR loop of the sample is shown in Fig. 4(c). As shown in Fig. 4(b), R_PA increases more rapidly for samples with t_{CoFeB}=2.7 and 4.3 nm than for sample with t_{CoFeB} =6.0 nm; although the mechanism is not fully transparent, the increased annealing temperature affects less the t_{CoFeB} =6.0 nm sample, in accordance with the Ta diffusion scenario. In another sample consisting of the same structure, TMR ratios of 576% at 300 K and 1144% at 5 K were observed.

In summary, we investigated the factors affecting the TMR ratios of CoFeB/MgO/CoFeB MTJs at high annealing temperatures above 500 °C. With an the increase in the annealing temperature, relaxation of residual stress and the improvement of the (001) orientation in 10-nm-thick MgO, deposited under the same sputtering conditions as the MgO barrier used in MTJs, took place. Cross-sectional HRTEM showed that Ta diffuses through the CoFeB electrode and reaches the MgO barrier. The suppression of Ta diffusion by employing a thick CoFeB electrode was found to result in a high TMR ratio of 604% at 300 K in a $Co_{20}Fe_{60}B_{20}/MgO/Co_{20}Fe_{60}B_{20}$ PSV MTJ annealed at 525 °C, and TMR ratios of 576% at 300 K and 1144% at 5 K in a different sample with the same film structure.

This work was supported in part by "High-Performance Low-Power Consumption Spin Devices and Storage Systems" program under Research and Development for Next-Generation Information Technology of MEXT. The authors wish to thank Y. Ohno, I. Morita, and T. Hirata for their technical support in MTJ fabrication and valuable discussions.

[1] S. Yuasa, A. Fukushima, T. Nagahama, K. Ando, and Y. Suzuki, Jpn. J. Appl. Phys., Part 2 **43**, L588 (2004); Nat. Mater. **3**, 868 (2004).
[2] S. S. P. Parkin, C. Kaiser, A. Panchula, P. M. Rice, B. Hughes, M. Samant, and S. H. Yang, Nat. Mater. **3**, 862 (2004).
[3] D. D. Djayaprawira, K. Tsunekawa, M. Nagai, H. Maehara, S. Yamagata, N. Watanabe, S. Yuasa, Y. Suzuki, and K. Ando, Appl. Phys. Lett. **86**, 092502 (2005).
[4] J. Hayakawa, S. Ikeda, F. Matsukura, H. Takahashi, and H. Ohno, Jpn. J. Appl. Phys., Part 2 **44**, L587 (2005).
[5] C. Tiusan, M. Sicot, M. Hehn, C. Belouard, S. Andrieu, F. Montaigne, and A. Schuhl, Appl. Phys. Lett. **88**, 062512 (2006).
[6] M. Hosomi, H. Yamagishi, T. Yamamoto, K. Bessho, Y. Higo, K. Yamane, H. Yamada, M. Shoji, H. Hachino, C. Fukumoto, H. Nagao, and H. Kano, Tech. Dig. - Int. Electron Devices Meet. **2005**, 459.
[7] Z. Diao, D. Apalkov, M. Pakala, Y. Ding, A. Panchula, and Y. Huai, Appl. Phys. Lett. **87**, 232502 (2005).
[8] T. Kawahara, R. Takemura, K. Miura, J. Hayakawa, S. Ikeda, Y. M. Lee, R. Sasaki, Y. Goto, K. Ito, T. Meguro, F. Matsukura, H. Takahashi, H. Matsuoka, and H. Ohno, IEEE ISSCC Digest of Technical Papers, 2007 (unpublished), p. 480; IEEE J. Solid-State Circuits **43**, 109 (2008).
[9] A. Mochizuki, H. Kimura, M. Ibuki, and T. Hanyu, IEICE Trans. Fundamentals **E88-A**, 1408 (2005).
[10] S. Ikeda, J. Hayakawa, Y. M. Lee, F. Matsukura, Y. Ohno, T. Hanyu, and H. Ohno, IEEE Trans. Electron Devices **54**, 991 (2007).
[11] S. Matsunaga, J. Hayakawa, S. Ikeda, K. Miura, H. Hasegawa, T. Endoh, H. Ohno, and T. Hanyu, Appl. Phys. Express **1**, 091301 (2008).
[12] W. H. Butler, X.-G. Zhang, T. C. Schulthess, and J. M. MacLaren, Phys. Rev. B **63**, 054416 (2001).
[13] J. Mathon and A. Umersky, Phys. Rev. B **63**, 220403R (2001).
[14] Y. M. Lee, J. Hayakawa, S. Ikeda, F. Matsukura, and H. Ohno, Appl. Phys. Lett. **90**, 212507 (2007).
[15] Y. M. Lee, J. Hayakawa, S. Ikeda, F. Matsukura, and H. Ohno, Appl. Phys. Lett. **89**, 042506 (2006).
[16] J. Hayakawa, Y. M. Lee, S. Ikeda, F. Matsukura, and H. Ohno, Appl. Phys. Lett. **89**, 232510 (2006).
[17] S. Ikeda, J. Hayakawa, Y. M. Lee, R. Sasaki, T. Meguro, F. Matsukura, and H. Ohno, Jpn. J. Appl. Phys., Part 2 **44**, L1442 (2005).
[18] M. G. Wang, C. Ni, A. Rumaiz, Y. Wang, X. Fan, T. Moriyama, R. Cao, Q. Y. Wen, H. W. Zhang, and J. Q. Xiao, Appl. Phys. Lett. **92**, 152501 (2008).
[19] S. Yuasa, Y. Suzuki, T. Katayama, and K. Ando, Appl. Phys. Lett. **87**, 242503 (2005).
[20] S. Ikeda, J. Hayakawa, Y. M. Lee, T. Tanikawa, F. Matsukura, and H. Ohno, J. Appl. Phys. **99**, 08A907 (2006).
[21] S. Cardoso, C. Cavaco, R. Ferreira, L. Pereira, M. Rickart, P. P. Freitas, N. Franco, J. Gouveia, and N. P. Barradas, J. Appl. Phys. **97**, 10C916 (2005).
[22] Y. Ashizawa, H. Ohyama, K. Sunaga, Y. Watanabe, M. Tsunoda, and M. Takahashi, J. Magn. Soc. Jpn. **31**, 411 (2007), in Japanese.
[23] F. M. D'Heurle, Metall. Trans. **1**, 725 (1970).